

Metal-Selective DNA-Binding Response of *Escherichia coli* NikR[†]

Stephanie L. Bloom and Deborah B. Zamble*

Department of Chemistry, University of Toronto, Toronto, Ontario, Canada M5S 3H6

Received March 26, 2004; Revised Manuscript Received May 21, 2004

ABSTRACT: The NikR transcription factor from *Escherichia coli* is a Ni(II)-dependent repressor that regulates production of the nickel ion transporter encoded by the *nik* operon. In the previous paper in this issue (Wang, S. C., Dias, A., Bloom, S. L., and Zamble, D. B. (2004) Selectivity of Metal Binding and Metal-Induced Stability of *Escherichia coli* NikR, *Biochemistry* 43, 10018–10028) we demonstrated that NikR can bind 1 equiv of Ni(II) or several other divalent transition metals with similar affinities, but that the Ni(II)-loaded protein is less susceptible to thermal or chemical denaturation than other divalent metal complexes. Here, we investigate the metal selectivity of the DNA-binding activity of NikR. Stoichiometric nickel induces binding of nanomolar NikR to the recognition sequence in the *nik* promoter, but single equivalents of other divalent metals such as Cd(II), Co(II), and Cu(II) also induce a similar DNA-binding affinity. In the presence of excess nickel, DNA-binding experiments indicate that NikR binds to the *nik* promoter as a tetramer with much higher affinity (20 pM), and it is this response that is selective for nickel. The DNA binding induced by an excess of other divalent metals is weaker, and is enhanced by the addition of stoichiometric nickel. Nickel titrations into a DNA-binding assay reveal a nickel affinity of 30 nM for a second metal-binding site, and in the presence of 30 nM metal only nickel induces detectable DNA binding by Ni(II)–NikR. These experiments support the hypothesis that there are two metal-binding sites and that both contribute to the nickel-selective DNA-binding response. A model for the in vivo activity of NikR is discussed.

Metalloregulators play a central role in the maintenance of healthy levels of both essential and toxic transition metals (1). They act as biomolecular sensors that monitor the cellular concentrations of metals and then adjust the expression of other components of the metal homeostasis pathways accordingly. Transcription factors have now been identified that specifically respond to one or more of over a dozen different metals (for reviews see refs 2–6). Allosteric regulation of many of these protein families is controlled by direct metal coordination to the protein and a concomitant conformational change that affects DNA binding. However, the details of the allosteric regulation are poorly understood. In addition, it is not clear how the proteins are able to discriminate between the physiologically available metals to achieve a metal-selective response.

The *Escherichia coli* (*E. coli*)¹ NikR protein is responsible for the nickel-mediated repression of the *nik* operon that encodes the nickel membrane transporter NikABCDE (7, 8). This 15 kDa protein is a member of the ribbon–helix–helix family of prokaryotic transcription factors (9) that includes the bacteriophage Arc and Mnt repressors and the methio-

nine-responsive MetJ (10, 11). NikR binds two dyad-symmetric repeat sequences that overlap the *nik* transcription start site (9, 12). The DNA-binding motif is composed of two intertwined monomers (13), and in analogy with other members of this family it is likely that the protein binds to the DNA as a pair of dimers (11). Biochemical experiments and structural analysis indicate that micromolar NikR exists as a tetramer, either with or without nickel bound (13, 14).

Each NikR tetramer can bind four nickel ions at sites that bridge the two DNA-binding dimers (13). How nickel binding to NikR induces DNA binding is not known, although the crystal structure of the apoprotein suggests that a significant conformational rearrangement must occur in the tetramer to accommodate binding to both of the DNA half-sites in the recognition sequence (13). In vitro studies demonstrated that NikR binds the *nik* promoter in response to stoichiometric amounts of nickel (14), but excess nickel produces a marked increase in the DNA affinity (12), suggesting that there are two levels of control (Figure 1). Whether one or both of the metal-binding responses are physiologically relevant or if either mediates a nickel-selective response are important issues that have not been resolved.

Although NikR binds stoichiometric nickel with picomolar affinity (14, 15), the protein also binds other divalent ions with a similar or even higher affinity (15). However, nickel stabilizes the folded structure of NikR more than any of the other metals, suggesting that there is a nickel-specific effect on the protein conformation. In this paper we examine the metal selectivity of the DNA-binding response of NikR. Our

[†] This work was supported by NSERC (Canada).

* To whom correspondence should be addressed. Phone: (416) 978-3568. E-mail: dzamble@chem.utoronto.ca.

¹ Abbreviations: DTNB, 5,5'-dithiobis(2-nitrobenzoic acid); DTT, dithiothreitol; *E. coli*, *Escherichia coli*; EDTA, ethylenediaminetetraacetic acid (disodium salt); EXAFS, extended X-ray absorption fine structure; HEPES, 4-(2-hydroxyethyl)-1-piperazineethanesulfonic acid; ICP-AES, inductively coupled plasma atomic emission spectroscopy; NTA, nitrilotriacetic acid; MSA, mobility-shift assay; PAGE, polyacrylamide gel electrophoresis; Tris, tris(hydroxymethyl)aminomethane.

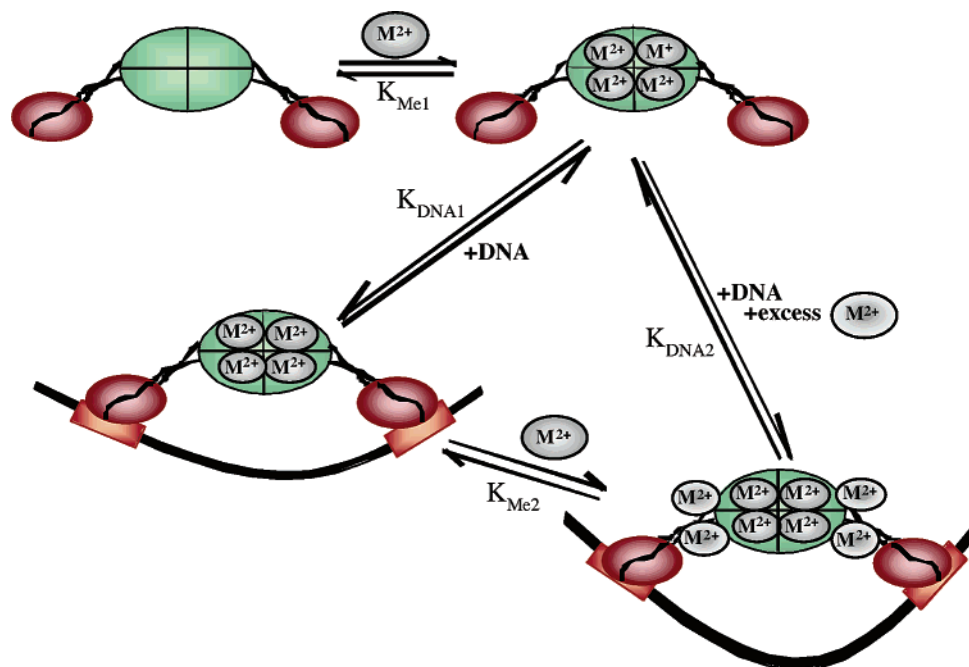


FIGURE 1: Model of the individual metal-binding and DNA-binding steps of NikR. M^{2+} represents a divalent metal, and the protein is drawn as a tetramer. Modified from ref 14.

experiments demonstrate that several divalent metals can produce a similar DNA-binding response when present in stoichiometric amounts. It is only in the presence of excess amounts of metal that the resulting protein–DNA complex exhibits nickel selectivity. Evidence is presented for a physiologically relevant second metal-binding site, and the metal selectivity for the DNA-binding activity induced by both metal-binding sites is investigated. The implications for the control of nickel homeostasis in *E. coli* are discussed.

EXPERIMENTAL PROCEDURES

Materials. Restriction endonucleases, kinases, and polymerases were obtained from New England Biolabs except for *Cla*I, which was purchased from MBI Fermentas. DNA oligonucleotides were purchased from Sigma Genosys. Chelex-100 was purchased from BioRad. Metal salts were a minimum of 99.9% pure and purchased from Aldrich. The concentrations of metal stocks prepared from these salts were confirmed by ICP-AES. All other reagents were molecular biology grade from Sigma except where noted. The plasmids pNIK103 and pPC163 were generously donated by P. Chivers (Washington University School of Medicine, St. Louis, MO) (12). Water was deionized on a Milli-Q water system (Millipore), and the pH of all Tris buffers was adjusted with HCl at room temperature. All data were fitted by using Kaleidagraph 3.0.

Protein Expression and Purification. The *E. coli* NikR protein was expressed from the plasmid pNIK103 transformed into BL21(DE3) or BL21(DE3)pLysS cells, and purified on a Ni–NTA column (Qiagen) as previously described (12), followed by anion exchange chromatography (15). The protein was characterized by mass spectrometry, the oxidation state was assessed by a DTNB assay, and the purified protein was shown to be apo by using ICP-AES, as described elsewhere (15).

Mobility-Shift Assays. Electrophoretic mobility-shift assays were performed with 7% native polyacrylamide gels contain-

ing 300 mM boric acid and 75 mM Tris in lieu of standard TBE. The same Tris–borate solution (final pH \approx 7.5) was used as running buffer, and the binding buffer contained 20 mM Tris (pH 7.5), 100 mM KCl, 3 mM $MgCl_2$, 0.1% IGEPAL, 5% glycerol, 0.1 mg/mL bovine serum albumin (Aldrich), and 0.1 mg/mL sonicated herring sperm DNA (Promega). Metal solutions were added to the binding buffer, running buffer, and the gel before polymerization, to final concentrations as noted.

A 100-bp DNA fragment containing the *nik* promoter was amplified by PCR from the pPC163 plasmid by using primers SB001 (5'-CGA CTG CCC ATC TAT TGA TCC AGA ACA GG) and SB002 (5'-GGT AAC CCC AAT GGA TTA AAA TAG ATG GCG). A nonspecific 98-bp DNA fragment was cloned from the same plasmid using primers SBnobind3 (5'-GAA AGA CGG TGA GCT GGT GAT ATG G-3') and SBnobind4 (5'-GGT ATT CAC TCC AGA GCG ATG AAA AC-3'). The nonspecific probe was selected to have the same T_m as the specific probe and a GC content similar to that of the specific probe. The PCR products were end-labeled with [γ - ^{32}P]ATP and T4 polynucleotide kinase, and unincorporated nucleotides were removed with a G-25 microspin column (Pharmacia). Typically, 5–25 pM (500–2000 cpm) DNA was incubated with NikR for at least 30 min at room temperature in 50 μ L of binding buffer except for in the experiments used to quantitate the DNA binding constant in the presence of nickel, in which less DNA was used. A 35 μ L portion of the reaction sample was loaded onto the gel without additional loading buffers or dyes, and the gel was run at 300 V and 4 $^{\circ}$ C. The gels were vacuum-dried and exposed to a phosphor screen, then scanned on a Molecular Dynamics Storm 860 phosphorimager, and analyzed with ImageQuant 5.0 software. All DNA-binding data sets were fitted to a Langmuir equation with a variable Hill coefficient n : $r = [NikR]^n / ((K_{d(app)})^n + [NikR]^n)$, where r is the fraction of DNA bound and $K_{d(app)}$ represents the protein concentration required for 50% binding. The maximum fraction of DNA

Table 1: Metal-Induced DNA Binding^a

Me(II)	1:1 Me(II)–NikR K_{DNA1}^b	excess Me(II) K_{DNA2}^c	1:1 Ni(II) + excess Me(II) ^c
Mn ²⁺	n/o ^d	$(2.4 \pm 0.1) \times 10^{-9}$ (1.4 ± 0.2)	$(5 \pm 1) \times 10^{-10}$ (1.4 ± 0.4)
Co ²⁺	$(1.1 \pm 0.2) \times 10^{-8}$ (2.1 ± 0.8)	$(1.4 \pm 0.4) \times 10^{-9}$ (0.9 ± 0.1)	$(4.8 \pm 0.8) \times 10^{-10}$ (1.7 ± 0.4)
Ni ²⁺	$(5 \pm 1) \times 10^{-9}$ (1.5 ± 0.5)	$(2.0 \pm 0.2) \times 10^{-11}$ (1.0 ± 0.1)	
Cu ²⁺	$(3 \pm 1) \times 10^{-9}$ (1.6 ± 0.2)	$(6 \pm 1) \times 10^{-10}$ (0.9 ± 0.2)	$(8 \pm 3) \times 10^{-11}$ (1.0 ± 0.3)
Zn ²⁺	$(2.7 \pm 0.4) \times 10^{-7}$ (1.2 ± 0.4)	n/d ^e	$\sim 5 \times 10^{-9}$, 2×10^{-7}
Cd ²⁺	$(1.8 \pm 0.2) \times 10^{-8}$ (1.8 ± 0.8)	$> 2.5 \times 10^{-8}$	$\sim 4 \times 10^{-9}$

^a The protein concentrations (M) of half-maximal binding are listed, with the estimated Hill coefficients from the data fitting indicated in parentheses. Average values from a minimum of two independent experiments are listed \pm standard deviation. ^b Determined by DNase footprinting. ^c Determined by MSA experiments with 35 μ M Me(II) in the gel and running buffer. ^d DNA binding was not observed in the DNase footprinting assay with stoichiometric Mn(II). ^e Not determined due to protein aggregation.

bound was not allowed to vary from 1 except where noted. The numbers reported are the averages and standard deviations from the fits of at least duplicate experiments.

DNase Footprinting. A 133-bp DNA probe was obtained from pPC163 by digesting the plasmid with *SaI*. The resulting 4-bp overhang was labeled with [α -³²P]dCTP by using the large Klenow fragment. The DNA was then desalted into buffer Y+/Tango (MBI Fermentas) and digested with *Bsu*15I (*Cla*I). The DNA fragment was purified by 7% native polyacrylamide gel electrophoresis followed by electroelution from the gel slice and ethanol precipitation. The amount of labeling was determined by scintillation counting on a Packard Tri-Carb 2900TR LSC instrument. The Maxam–Gilbert chemical sequencing G reaction was performed by using standard protocols (16).

The DNase footprinting reactions were carried out in 20 μ L volumes and contained Chelex-treated 100 mM KCl and 10 mM HEPES, pH 7.6, as well as 100 μ g/mL BSA, 1 mM MgCl₂, 5% (v/v) glycerol, and 100–300 pM ³²P-labeled probe (\sim 30000–80000 cpm/sample). Metal salts and NikR were added as noted. The samples were incubated at room temperature for 1 h prior to the addition of 1 μ L of 2 μ g/mL DNase I (Roche). The reactions were quenched after 1–2 min by the addition of 75 μ L of DNase stop buffer (20 mM EDTA, pH 8.0, 200 mM NaCl, 1% (w/v) SDS, 125 μ g/mL yeast tRNA). Following extraction with 100 μ L of 24:25:1 phenol/chloroform/isoamyl alcohol, the DNA was precipitated with ethanol/sodium acetate. The DNA pellets were resuspended in 4 μ L of formamide loading buffer (16), denatured at 90 °C for 5 min, and loaded onto an 8% denaturing polyacrylamide gel prerun to 50 °C in TBE. The gels were run at \sim 2000 V, vacuum-dried, and then analyzed on the phosphorimager. Each lane was normalized to account for sample loading by the comparison of several reference bands which were unaffected by protein binding to the same bands in the control sample. The degree of protection was then determined by quantitation of the intensity of two bands within the binding sequence. Half-maximal binding was calculated by fitting the data as described for the mobility-shift assays.

RESULTS

DNA Binding Induced by Stoichiometric Metal. NikR can bind several divalent transition metals other than nickel, such as Zn(II), Cd(II), Cu(II), and Co(II), with affinities that are similar to or stronger than that of nickel binding (15). However, nickel stabilizes NikR to the largest extent, and it is unlikely that the other metals are all bound in the same square-planar geometry observed for nickel (13, 17, 18).

Thus, it is possible that there is a nickel-specific conformational change in NikR that leads to DNA binding.

To test this hypothesis, the metal selectivity of the DNA-binding response of NikR to stoichiometric metal was examined. DNase footprinting experiments were performed with a DNA probe containing the *nik* operator (12, 14). The buffer components were pretreated with Chelex to minimize adventitious metal contamination. No protection of the DNA from DNase digestion was observed with up to 2 μ M apo-NikR or with protein in the presence of stoichiometric MnCl₂ (data not shown). Upon the addition of 1 equiv of Ni(II), NikR bound to the DNA and produced a footprint at the binding sites around the transcription start site (Figure 2) as previously reported (12, 14). One equivalent of Cu(II), Cd(II), Zn(II), or Co(II) also produced a similar footprint (Figure 2). Both the Ni(II)-bound NikR and the Cu(II)-bound protein protect the DNA with comparable half-maximal affinities (K_{DNA1}) of 5 ± 1 and 3 ± 1 nM, respectively (Figure 2B and Table 1). DNA binding was only slightly weaker with stoichiometric Cd(II) and Co(II). Upon incubation with stoichiometric zinc, protection of the DNA probe was not complete even at the maximum protein concentration used (1 μ M), but the data could be fitted with a half-maximal binding affinity of $(2.0 \pm 0.3) \times 10^{-7}$ M (Figure 2B and Table 1). For all of the metals, the data were fitted with Hill coefficients close to 1.5, suggesting that there may be a small degree of cooperativity as NikR binds to the DNA. These DNase footprinting experiments are based on the assumption that 1 equiv of metal will all be bound to the protein. If the metal affinity of the protein does not significantly change when it binds DNA, then this assumption is reasonable for the high picomolar to mid-nanomolar protein concentrations used in the presence of nickel, copper, zinc, or cadmium (15). However, because both cobalt and manganese have weaker affinities for NikR, it is possible that the metal is not completely bound to the protein in these experiments and the DNA affinity of these metal complexes is underestimated.

DNA Binding in the Presence of Excess Metal. The mobility-shift assay (MSA) was used as a complementary method to examine NikR binding to a 100-bp probe containing the *nik* promoter region. In contrast to the DNase footprinting experiments, as reported by Chivers et al. (12), DNA binding was not observed in the MSA experiments if NikR was incubated with only stoichiometric amounts of metal (data not shown). Instead, DNA binding was detected in the presence of a constant excess (μ M) of metal in the gel and electrophoresis buffer (Figure 3). It is unclear at this time why the DNA complex formed in the presence of

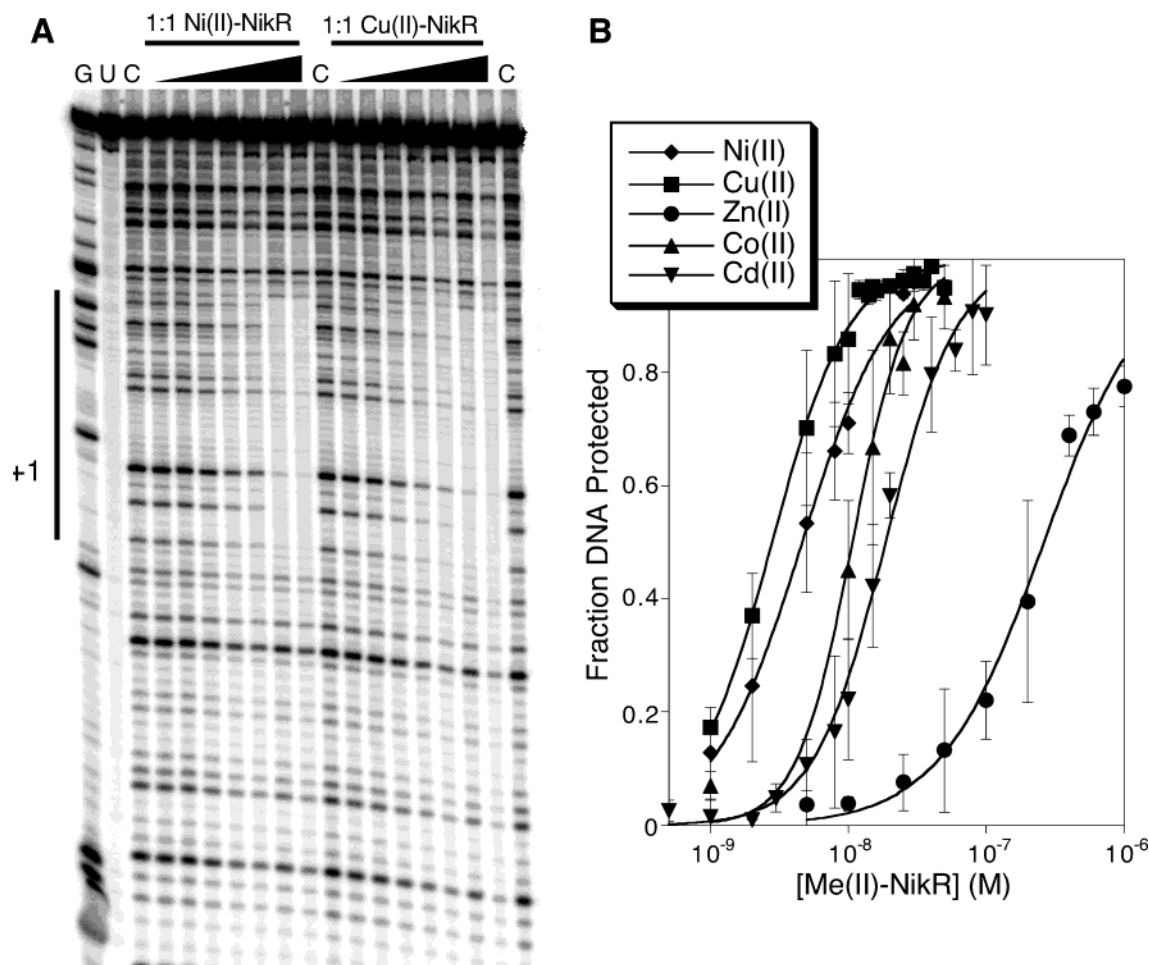


FIGURE 2: DNA binding of NikR with stoichiometric metal. (A) Increasing concentrations of NikR were incubated with stoichiometric Ni(II) or Cu(II) and the 133-bp DNA probe for 1 h at room temperature prior to the addition of DNase I and analysis on an 8% denaturing polyacrylamide gel. The transcription start site and area of protection are indicated. Key: G, Maxam–Gilbert G reaction; U, undigested probe; C, control DNase reaction without any NikR but with the maximum amount of metal used. (B) DNA binding by NikR was examined in the presence of Ni(II), Cu(II), Co(II), Cd(II), and Zn(II). The error bars indicate standard deviations between at least two footprinting experiments such as those shown in panel A. The data were fitted to a Hill binding equation as described in the Experimental Procedures, and the binding constants are listed in Table 1.

1 equiv of metal is not detected by MSA, although it is interesting to note that MSA experiments with the homologous MetJ were also performed with constant concentrations of the positively charged cofactor *S*-adenosylmethionine in the gels (19). To determine the stoichiometry of the protein–DNA complex, MSA experiments were performed with a DNA concentration several orders of magnitude larger than the apparent $K_{\text{DNA}2}$ for the complex formation in the presence of excess nickel (12; see also below). In the presence of 50 nM DNA and 35 μM nickel, a ratio of almost four protein molecules for each DNA molecule was required to titrate the binding site (Figure 3A). This experiment suggests that NikR binds to the operator as tetramer, an observation consistent with the activity of other members of the ribbon–helix–helix family (10). This association is not a general metal-induced effect because DNA binding was not observed under the same conditions with an oligonucleotide of the same length and GC content but without the NikR binding sequence (Figure 3B).

In the presence of excess nickel, the apparent K_d for the protein–DNA complex ($K_{\text{DNA}2}$) is 20 pM (Figure 4, Table 1), in good agreement with that from a previous study (12), and much lower than that observed with just stoichiometric metal ($K_{\text{DNA}1}$, Figure 2). The affinity for DNA was about

30-fold weaker in the presence of excess Cu(II) and several orders of magnitude weaker for Co(II) and Mn(II) (Figure 4 and Table 1). In the presence of excess Zn(II) and Cd(II), protein precipitation prevented an accurate measurement of the binding affinity, although a lower limit could be estimated with cadmium (Table 1). For these experiments, excess metal was present in the gel and buffer but was not preincubated with the protein–DNA sample prior to loading on the gel to avoid protein precipitation. Preincubation with nickel did not affect the apparent $K_{\text{DNA}2}$ of DNA binding, indicating that the metal in the gel buffer was sufficient to induce DNA binding (data not shown). Finally, preliminary experiments suggest that excess Ca^{2+} can also induce DNA binding with a half-maximal binding affinity of ~ 10 nM (data not shown).

The observation that excess nickel increases the affinity of NikR for its recognition sequence above that observed with just 1 equiv of nickel supports the hypothesis that there are two metal-binding sites on NikR with different affinities (14). To test whether having nickel bound in the high-affinity site would influence the DNA binding induced by an excess of a different metal, the protein was first incubated with 1 equiv of nickel. NikR binds stoichiometric nickel with picomolar affinity (14, 15), and these MSA experiments are performed with protein concentrations several orders of

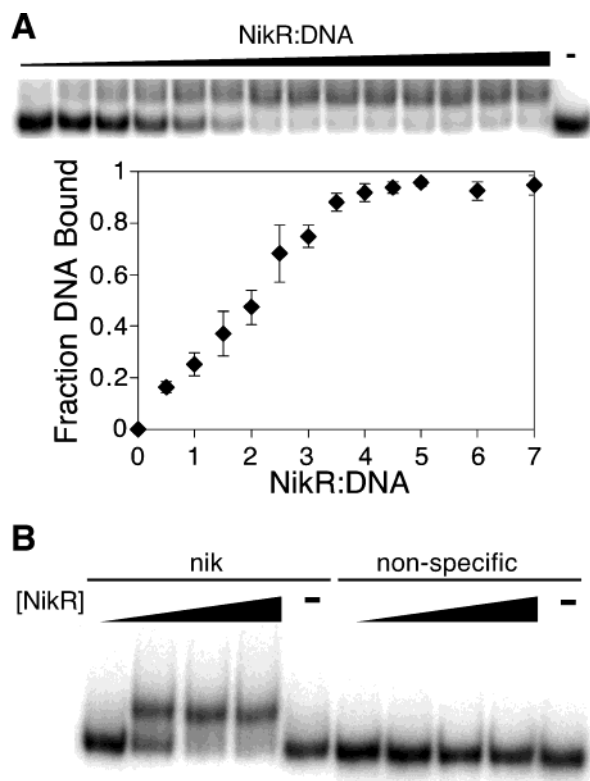


FIGURE 3: DNA binding in the presence of excess nickel. (A) NikR (25–500 nM) was incubated with 50 nM DNA in the presence of 35 μ M NiSO₄. The reactions were analyzed on a 7% native gel with 35 μ M NiSO₄ in the gel and running buffer. The data plotted (just up to 7 equiv, for clarity) are from duplicate experiments such as that shown above; the error bars indicate standard deviations. (B) NikR (10 pM to 1 μ M) was incubated with a 2 nM concentration of a DNA probe containing either the operator recognition sequence (nik) or a randomly selected sequence (non-specific) in the presence of 35 μ M NiSO₄. The reactions were analyzed on a 7% native gel with 35 μ M NiSO₄ in the gel and running buffer.

magnitude higher so essentially all of the nickel will be bound to the high-affinity metal site. For each of the additional metals analyzed, stronger DNA binding was observed when the protein was first incubated with stoichiometric amounts of nickel (Figure 5A, Table 1). Weak DNA binding was even detected in the presence of Zn(II) if the protein was preincubated with stoichiometric amounts of nickel (Figure 5B), suggesting that under these conditions nickel protects the protein from aggregation. In the zinc experiments, two distinct complexes were observed. The faster mobility complex exhibits the same shift as that observed with all of the other metals. A second, slower mobility complex was also observed, most likely due to a higher order protein complex, but this complex has not yet been characterized.

The addition of stoichiometric nickel to NikR prior to performing an MSA experiment enhances the DNA binding induced by a variety of metals, indicating that nickel bound to the high-affinity site affords a degree of metal selectivity. To provide additional support for the two-site model, experiments were performed in which Ni(II)–NikR was incubated with Cu(II) for different lengths of time. NikR binds stoichiometric copper much tighter than nickel (15), so at equilibrium the copper should be able to replace nickel in the high-affinity site and weaker DNA binding should be

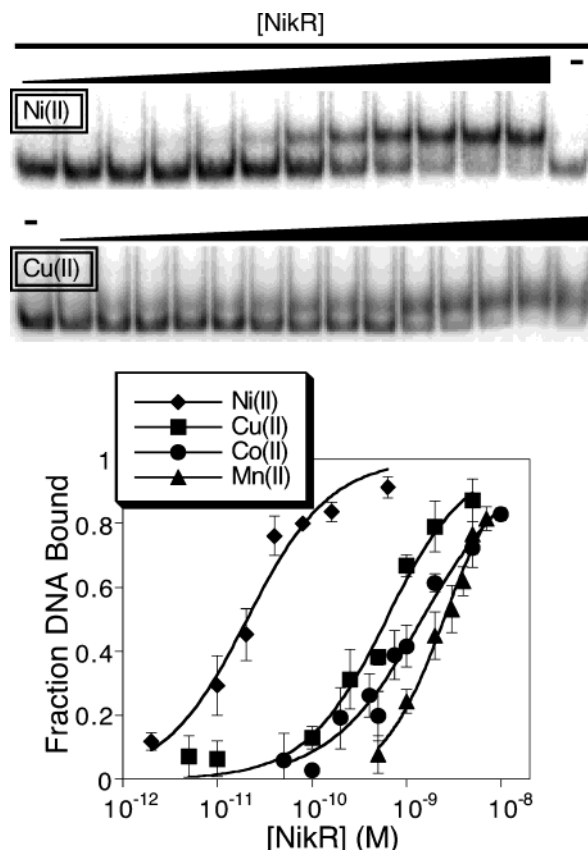


FIGURE 4: Metal selectivity of high-affinity DNA binding. NikR was incubated with the 100-bp *nik* DNA followed by analysis on 7% native gels in the presence of 35 μ M Ni(II), Cu(II), Co(II), or Mn(II). The data were fitted to a Hill binding equation as described in the Experimental Procedures, and the binding constants are listed in Table 1. Error bars indicate standard deviations of at least two experiments such as those shown for Ni(II) and Cu(II) in the top panel.

observed. An example of such an experiment is shown in Figure 5C. In the top gel, excess copper (50 μ M) was added to the Ni(II)–NikR complex just prior to loading the gel and half-maximal DNA binding is observed at 6×10^{-11} M. If the Ni(II)–NikR complex is first incubated for 16 h with the excess copper (Figure 5C, bottom gel), weaker DNA binding is observed with a half-maximal binding affinity of 0.7 nM. This DNA-binding affinity is similar to that detected with only copper present (Table 1), demonstrating that the copper is indeed replacing the nickel in the high-affinity site and producing weaker DNA binding.

Titration of the “Low-Affinity” Metal-Binding Site. The concentration of protein required for half-maximal DNA binding in the presence of 1 equiv of metal is 5 nM (K_{DNA1}), but a micromolar excess of metal reduces this number to 20 pM (K_{DNA2}). To isolate the effect of the excess metal on DNA binding by NikR, nickel was titrated into DNase footprinting samples containing NikR and stoichiometric nickel. To detect the effects of the additional metal, the concentration of protein had to be larger than K_{DNA2} but below K_{DNA1} . The ratio of protein to DNA was also important for this analysis. If the NikR concentration was higher than the DNA concentration, the DNA protection would saturate with only a fraction of the available protein, resulting in an underestimate of the required metal concentration. Conversely, if the protein concentration was too low, the intensity of the

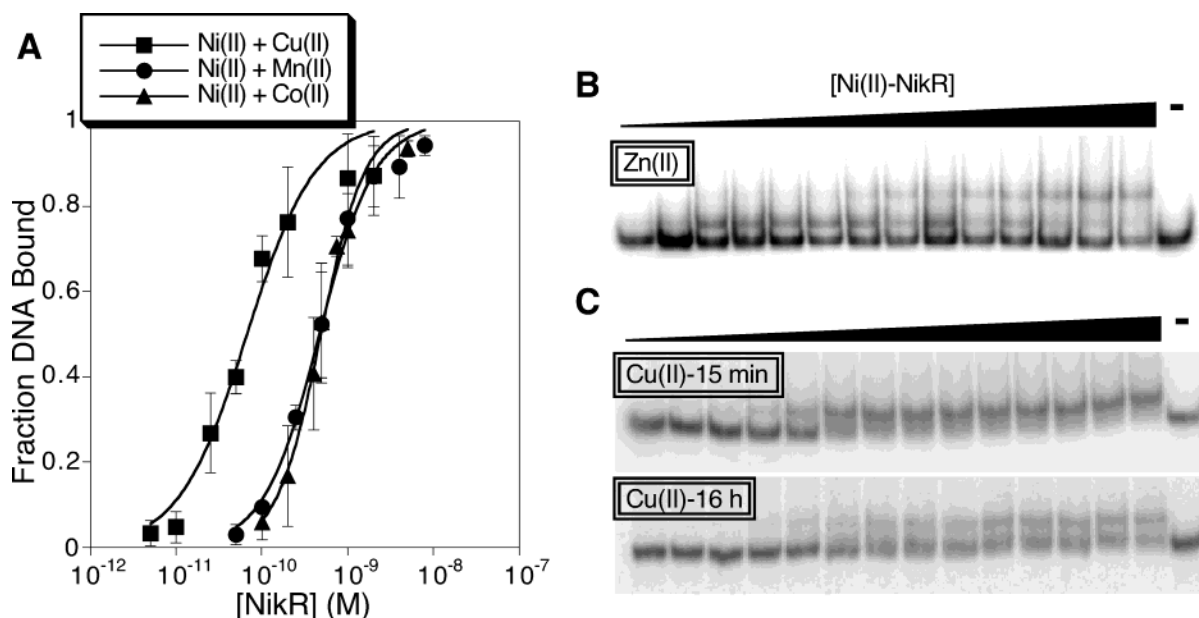


FIGURE 5: DNA binding of Ni(II)–NikR in the presence of excess metal. (A) Ni(II)–NikR was incubated with the 100-bp *nik* DNA probe followed by analysis on a 7% native gel in the presence of 35 μ M Cu(II), Mn(II), or Co(II). The data were analyzed as described in the Experimental Procedures, and the binding constants are listed in Table 1. Error bars indicate standard deviations of at least two experiments. (B) Ni(II)–NikR (500 pM to 2 μ M) was incubated with the 100-bp *nik* DNA probe followed by analysis on a 7% native gel in the presence of 20 μ M ZnSO₄. (C) Ni(II)–NikR (1 pM to 5 nM) was incubated with the 100-bp *nik* DNA probe and 50 μ M CuSO₄ for 15 min (top) or 16 h (bottom) prior to analysis on a 7% native gel in the presence of 50 μ M CuSO₄. The same protein concentrations were used in both experiments. The protein concentration required to reach half-maximal DNA binding increased from 0.06 to 0.7 nM.

footprint would be too weak even when all of the protein was metal- and DNA-bound. The MSA experiments indicate that NikR binds DNA as a tetramer (Figure 3A), so a stoichiometry of 4:1 protein:DNA was maintained. The concentration of DNA was first determined by titrating NikR with the DNA in the presence of a large excess of NiSO₄ at concentrations of DNA that were well above the K_{DNA2} of 20 pM (data not shown). In this experiment maximal saturation was achieved when the active protein concentration was equivalent to 4 times the DNA concentration.

Titration of nickel into reactions containing 1 nM Ni(II)–NikR and 250 pM DNA revealed half-maximal DNA binding at a nickel concentration (K_{Me2}) of $(2.9 \pm 0.3) \times 10^{-8}$ M (Figure 6), providing an estimate for the nickel affinity of the low-affinity metal-binding site (K_{Me2}). The extended footprint reported in another study was not observed (14) and the affinity reported here is tighter. It is not clear at this time what factor causes the discrepancy between these two studies.

To confirm that a low-affinity metal-binding site was inducing tight DNA binding, some additional MSA experiments were performed. Reducing the concentration of nickel from 35 to 1 μ M did not produce any detectable difference in DNA-binding affinity (data not shown). If only 1 nM Ni(II) was used in the experiment, however, the protein concentration required for half-maximal binding increased (Figure 7). At this lower nickel concentration the DNA binding did not completely saturate, so the data were fitted to a 70% saturation curve and the protein concentration for half-maximal binding was calculated to be 0.8 ± 0.3 nM NikR with a Hill coefficient of 1.1 ± 0.2 . This number correlates with that from the DNase footprinting experiments. If the metal affinity of the low-affinity site is 30 nM, then only about 3% of those sites will be filled at 1 nM metal and the protein concentration required for half-maximal

binding should be 30-fold that observed with 35 μ M nickel (20 pM, Table 1). This argument is based on the assumption that only protein in which the putative low-affinity second site is filled with nickel will produce DNA binding in this assay. Furthermore, the apparent affinity of the low-affinity metal-binding site (K_{Me2}) measured in both types of DNA-binding experiments is for the protein tetramer. The number of metal ions needed in the tetramer low-affinity sites to induce the tight DNA binding could not be measured because that experiment would require concentrations much higher than K_{Me2} , and at these protein concentrations stoichiometric metal is sufficient to induce DNA binding. Direct measurements of the metal binding to the low-affinity site will be required to measure the stoichiometry and to confirm this estimation of the dissociation constant.

To analyze the metal selectivity of the DNA-binding response to this second metal, both DNase footprinting and MSA experiments were performed. Titration of up to micromolar concentrations of Zn(II), Mn(II), or Co(II) into the DNase experiments performed with 1 nM NikR did not produce a detectable footprint (data not shown). The Cu(II) titration did result in partial protection of the DNA when low micromolar metal was used (data not shown), but the data were not sufficient to estimate an affinity constant because higher metal concentrations started to inhibit the DNase reaction. MSA experiments were also performed with lower concentrations of metals other than Ni(II). With 30 nM Mn(II), Cd(II), Co(II), or Zn(II), no DNA binding was observed in samples with up to 5 μ M protein (data not shown). Furthermore, the addition of stoichiometric nickel did not produce DNA binding under these conditions. Only 30 nM Cu(II) was able to induce DNA binding, with about 10% of the DNA bound by 500 nM protein in the absence of nickel and 30% bound in the presence of stoichiometric nickel. Finally, to test the effects of Ca²⁺ on DNA binding

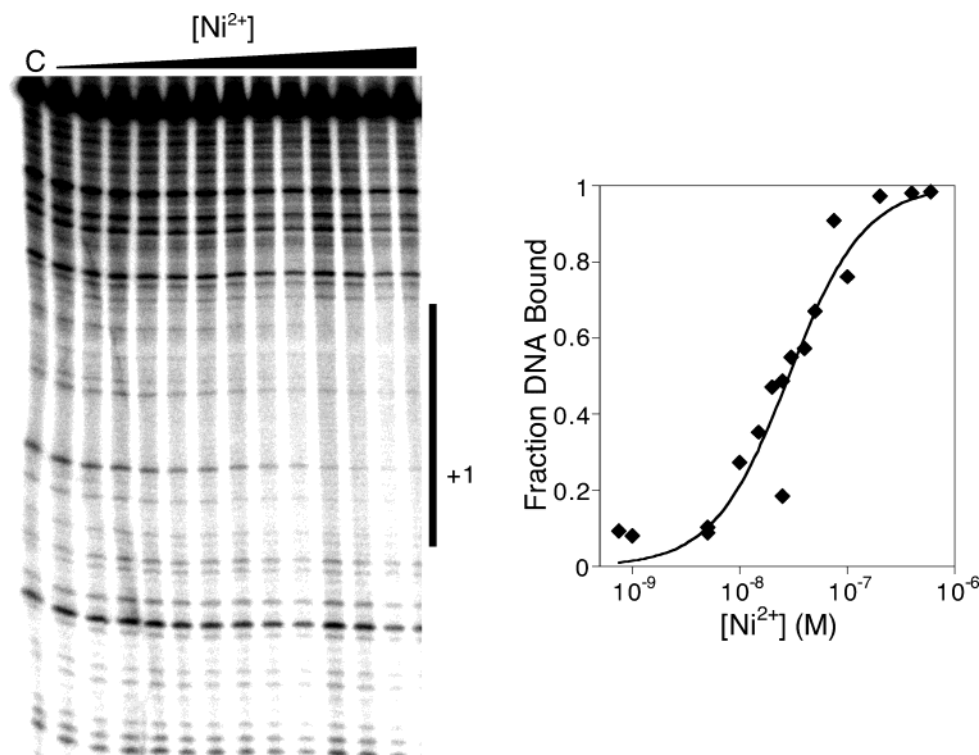


FIGURE 6: Low-affinity nickel-binding site. Increasing concentrations of NiSO_4 were added to reactions containing 1 nM NikR and 250 pM DNA prior to the addition of DNase I and analysis on denaturing PAGE. The data were compiled from two separate experiments and were fitted to a Hill binding curve as described in the Experimental Procedures, with a $K_{d(\text{app})}$ ($K_{\text{Me}2}$) of $(2.9 \pm 0.3) \times 10^{-8}$ M and a Hill coefficient of 1.2 ± 0.2 . C, control DNase reaction without any NikR but with the maximum amount of metal used.

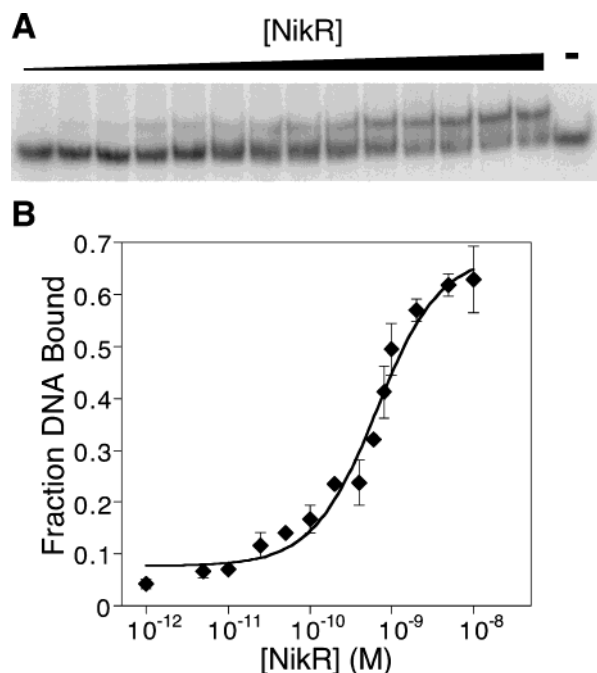


FIGURE 7: DNA binding in the presence of 1 nM Ni(II). (A) NikR (1 pM to 10 nM) was incubated with the 100-bp *nik* DNA probe followed by 7% native PAGE in the presence of 1 nM NiSO_4 . (B) Data from 1 nM Ni(II) MSA experiments such as the one shown in panel A were fitted to a Hill binding curve with a maximum saturation of 70% DNA bound. A $K_{d(\text{app})}$ of $(0.8 \pm 0.3) \times 10^{-9}$ M and a Hill coefficient of 1.1 ± 0.2 were calculated from analysis of two experiments such as that shown. The error bars indicate standard deviations of the duplicate experiments.

by NikR, MSA experiments were performed with 100 nM Ca^{2+} , the estimated concentration of free calcium in an *E. coli* cell (20). Under these conditions, only 25% of the

DNA was shifted in the presence of 50 nM Ni(II)–NikR (data not shown).

Another possible explanation for the apparent increase in DNA-binding affinity in the presence of extra metal is that there is only one metal-binding site on the protein but that the metal affinity changes upon formation of the complex with DNA. An EXAFS study revealed that the ligand coordination sphere around the nickel changes dramatically upon addition of DNA containing the recognition sequence (18). However, DNase footprinting experiments performed with DNA concentrations lower than the $K_{\text{Me}2}$ for the low-affinity nickel site saturate with approximately four protein molecules to one DNA molecule in the presence of only 1 equiv of nickel, indicating that the “high-affinity” metal site is maintained (data not shown). Furthermore, our preliminary experiments with a metallochromic indicator did not reveal any detectable change in nickel affinity in the presence of DNA (S. Wang, D. Zamble, unpublished data).

DISCUSSION

The experiments described here were designed to test the metal selectivity of the DNA-binding response of the *E. coli* metalloregulator NikR. The results support the hypothesis that there are two distinct metal-binding sites that regulate two levels of DNA binding (Figure 1). Furthermore, these results reveal that both sites provide a degree of metal selectivity for nickel, but that the metal selectivity is only apparent in the DNA-binding response to filling both sites.

NikR controls the transcription of a nickel transporter (8), so it is reasonable to expect that the protein would be selective for nickel. NikR binds one nickel ion per monomer with picomolar affinity (14, 15), and nickel induces DNA

binding to the regulator sequence (12). An examination of the metal-binding activity of NikR, however, revealed that the protein binds several different divalent metals such as Zn(II), Cd(II), and Cu(II), at least as tightly as nickel (15). We hypothesized that the metal-binding site was flexible and that, of the different metals examined, only the binding of Ni(II) ions (and possibly Cu(II)) would organize the protein into the appropriate conformation for DNA binding. This hypothesis was supported by denaturation experiments that revealed a selective enhancement of the secondary structure stability in the presence of nickel. However, the experiments reported here demonstrate that the metal-selective DNA-binding response of NikR is more complex.

The mechanism of metal-induced DNA binding is not yet known. The crystal structure of apo-NikR suggests that metal binding by the C-terminal domain must produce a significant change in the conformation of the tetramer to promote DNA binding to the *nik* operator (13). The fact that several transition metals produce a NikR complex with similar moderate affinities for the *nik* promoter suggests that the protein rearrangement is not constrained by the coordination preferences of any given ion. Instead, this observation suggests that stoichiometric divalent metal ions induce the same gross conformational changes in the protein. This hypothesis would explain why a square-planar ligand geometry is not maintained around 1 equiv of nickel upon DNA binding (18). It is tempting to speculate that high-affinity metal binding is responsible for stabilizing the quaternary structure of the protein. This metal-binding site bridges two DNA-binding dimers (18), and the protein binds to the DNA as a tetramer with a small degree of cooperativity. Analysis of the apoprotein both in solution and in the solid phase indicated that it forms a tetramer even in the absence of metal (14, 18), but these experiments were performed with protein concentrations several orders of magnitude higher than that required for half-maximal DNA binding. Additional studies are needed to analyze the quaternary structure of NikR at functional protein concentrations.

The lack of a metal selectivity in the DNA-binding response to stoichiometric metal is surprising given the role of NikR as a regulator of nickel uptake (8). It is possible that a metal-specific response by NikR is not necessary, if only nickel metal ions are available in the cytosol during the metabolic conditions in which NikR plays a critical role. Recent studies of pairs of homologous repressors revealed that in vivo transcriptional regulation can be controlled by the cytosolic availability of different metals (21, 22). However, a nickel-selective DNA response of NikR is observed with more than 1 equiv of metal, and thus, it may be that this second level of regulation is an important factor for the physiological role of NikR.

In the presence of excess metal, filling the second site with nickel strengthens the DNA affinity from 5 nM to 20 pM, an affinity on par with that of the homologous ribbon-helix-helix repressor Mnt (23). The DNA-binding activity induced by excess metal is selective for nickel. The only metal complex with a DNA-binding affinity that even approaches that of nickel is the 30-fold weaker Cu(II) complex. Whether the Cu(II) binding has any physiological relevance is unclear, since the intracellular copper ions that are not protein-bound are probably Cu(I) in the reducing environment of the cell (24, 25).

The metal selectivity of the high-affinity DNA-binding activity of NikR is produced by a combination of the properties of both metal-binding sites. The presence of stoichiometric nickel strengthens the DNA binding observed with an excess of any other metal, so the high-affinity metal-binding site does afford some metal selectivity. However, it is in filling the second metal site that the metal selectivity of NikR is most striking. In the presence of a 30 nM concentration of any transition metal other than nickel, only Cu(II) produced any detectable DNA binding in the MSA experiments with 500 nM protein, even if stoichiometric nickel was included. Furthermore, if the metals were titrated into the DNase footprinting experiment, only nickel ions induced DNA binding tight enough to protect the recognition sequence when the NikR concentration was lower than the K_{DNA1} , the DNA affinity of the 1:1 metal-protein complex, suggesting that metal binding to the second site is selective for nickel. Physiological levels of Ca(II), another ion that can induce DNA binding, also produced a DNA affinity that was several orders of magnitude weaker than that observed with 1 nM Ni(II).

The location of the second metal-binding site on NikR has not yet been established. The alignment of NikR homologues does not reveal a second set of conserved metal-binding ligands (9), and spectroscopic studies are constrained by protein precipitation. Upon close examination of the crystal structure (13) several locations on the protein stand out. There is an HHHD sequence following the H76 ligand of the high-affinity site on a surface loop close to H92' of the opposing monomer. There is also a cluster of metal-binding residues, composed of H123, H125, and C128', on the surface of the metal-binding domain that faces the DNA-binding domain. This cluster could then interact with helix 2 of the DNA-binding domain, which was highlighted by Schreiter et al. as a likely component of signal propagation because of its high degree of sequence conservation (13). Another nonexclusive model is that the second metal-binding site only exists in the protein when it forms a complex with DNA. Our preliminary experiments indicate that the protein precipitation observed with micromolar concentrations of NikR in the presence of excess metal is not observed when DNA is added (S. Wang, D. Zamble, unpublished data). The possibility that the DNA itself plays a role in the low-affinity site, as recently proposed for a nickel-bridging RNA-amino acid complex (26), also cannot be ruled out. Experiments to directly measure the metal affinity of the second site and determine its location are under way.

Other metalloregulators have more than one distinct metal-binding site. The cyanobacterial zinc sensor SmtB has two sites with at least a 20-fold difference in affinity for zinc (27, 28). Zinc binding to one type of site regulates DNA binding, but filling the higher affinity site does not, and it was postulated that this site has a different regulatory role (29). The iron-responsive Fur and the related zinc repressor Zur also bind two metal ions (30–32). Both proteins have a high-affinity zinc site, and it was suggested that this site serves a structural purpose while the second site is responsible for the metal-dependent allosteric control. The diphtheria toxin repressor (DtxR) from *Corynebacterium diphtheriae* is another iron-sensitive metalloregulator that has two metal-ion-binding sites (33), and while one site is essential for the DNA-binding response (33), the second ancillary site pro-

vides a cooperative enhancement to the metal sensitivity of the response (34).

Two metal-binding sites on NikR that modulate DNA binding are indicative of two levels of regulatory control. Whether or not a second site is a component of the *in vivo* activity of NikR is a question of debate (14, 35). The detection of nickel selectivity only at the second level of control suggests that it may be physiologically relevant to this regulator of nickel homeostasis. If our indirect measurement of a 30 nM nickel-binding affinity for this second site is accurate, then it is at a feasible concentration for intracellular regulation. At this time it is not known how much nickel is freely available in an *E. coli* cell growing under anaerobic conditions. However, Chivers et al. estimated that there are at least 125 molecules of NikR in an anaerobic *E. coli* cell (14). At an estimated maximum cell volume of 3.5 fL (36), four nickel ions per cell translates into a concentration of 2 nM, a metal concentration that would be sufficient to fill the second sites of four NikR molecules and induce tight DNA binding. A similar scenario has been proposed for *E. coli* Fur, which is purified with a tightly bound Zn(II) ion and is thought to exist as a Zn(II) complex *in vivo* (31). The Zn(II)–Fur complex in the absence of iron binds to a Fur box *in vitro* with a moderate K_d of 20 nM (31), but binding to the same site *in vivo* is only detected if the cells are grown in excess iron (37), suggesting that only filling the second metal site produces sufficient affinity to produce a response *in vivo*.

Thus, it is possible that the high-affinity metal-binding site of NikR is not the main regulator of nickel transporter expression. Stoichiometric metal binding is sufficient to induce moderate DNA binding, but whether this interaction affects transcription of the *nik* operon *in vivo* has not yet been established. Given the promiscuous nature of this activity, it would appear to be an unusually leaky mechanism as the sole control of a metal homeostatic pathway. Furthermore, the extremely high affinity of the first metal-binding site means that NikR would be in active competition with the proteins with a functional requirement for nickel ions. Perhaps binding stoichiometric metal serves to localize NikR to the *nik* promoter, where it may or may not play a regulatory role, and primes the protein to be ready to accept the second metal. If the intake of nickel then outpaced the cellular need, an overflow of a few nickel ions would be sufficient to induce very tight DNA binding and shut down production of the nickel transporter. The excess NikR molecules in the cell could then serve as a nickel buffer that protects the cell from the metal's toxic effects and stores the ions for future use.

ACKNOWLEDGMENT

We thank Prof. Peter Chivers for the generous donation of the pNIK103 and pPC163 plasmids, as well as for advice. We are also grateful to Profs. A. Woolley, R. Kluger, and C. Drennan as well as members of the Zamble laboratory for helpful discussions.

REFERENCES

- O'Halloran, T. V. (1993) Transition metals in control of gene expression, *Science* 261, 715–725.
- Winge, D. R., Jensen, L. T., and Srinivasan, C. (1998) Metal-ion regulation of gene expression in yeast, *Curr. Opin. Chem. Biol.* 2, 216–221.
- Outen, F. W., Outen, C. E., and O'Halloran, T. V. (2000) in *Bacterial Stress Responses* (Storz, G., and Hengge-Aronis, R., Eds.) pp 145–154, ASM Press, Washington, DC.
- Brown, N. J., Stoyanov, J. V., Kidd, S. P., and Hobman, J. L. (2003) The MerR family of transcriptional regulators, *FEMS Microbiol. Rev.* 27, 145–163.
- Busenlehner, L. S., Pennella, M. A., and Giedroc, D. P. (2003) The SmtB/ArsR family of metalloregulatory transcriptional repressors: structural insights into prokaryotic metal resistance, *FEMS Microbiol. Rev.* 27, 131–143.
- Finney, L. A., and O'Halloran, T. V. (2003) Transition metal speciation in the cell: insights from the chemistry of metal ion receptors, *Science* 300, 931–936.
- Wu, L. F., and Mandrand-Berthelot, M. A. (1986) Genetic and physiological characterization of new *Escherichia coli* mutants impaired in hydrogenase activity, *Biochimie* 68, 167–179.
- De Pina, K., Desjardin, V., Mandrand-Berthelot, M.-A., Giordano, G., and Wu, L.-F. (1999) Isolation and characterization of the *nikR* gene encoding a nickel-responsive regulator in *Escherichia coli*, *J. Bacteriol.* 181, 670–674.
- Chivers, P. T., and Sauer, R. T. (1999) NikR is a ribbon-helix-helix DNA-binding protein, *Protein Sci.* 8, 2494–2500.
- Knight, K. L., Bowie, J. U., Vershon, A. K., Kelley, R. D., and Sauer, R. T. (1989) The Arc and Mnt Repressors, *J. Biol. Chem.* 264, 3639–3642.
- Phillips, S. E. V. (1994) The β -ribbon DNA recognition motif, *Annu. Rev. Biophys. Biomol. Struct.* 23, 671–701.
- Chivers, P. T., and Sauer, R. T. (2000) Regulation of high affinity nickel uptake in bacteria, *J. Biol. Chem.* 275, 19735–19741.
- Schreiter, E. R., Sintchak, M. D., Guo, Y., Chivers, P. T., Sauer, R. T., and Drennan, C. L. (2003) Crystal structure of the nickel-responsive transcription factor NikR, *Nat. Struct. Biol.* 10, 794–799.
- Chivers, P. T., and Sauer, R. T. (2002) NikR repressor: high-affinity nickel binding to the C-terminal domain regulates binding to operator DNA, *Chem. Biol.* 9, 1141–1148.
- Wang, S. C., Dias, A., Bloom, S. L., and Zamble, D. B. (2004) Selectivity of metal binding and metal-induced stability of *Escherichia coli* NikR, *Biochemistry* 43, 10018–10028.
- Sambrook, J., and Russell, D. W. (2001) *Molecular cloning: A laboratory manual*, 3rd ed., Cold Spring Harbor Laboratory Press, Plainview, NY.
- Rulísek, L., and Vondrášek, J. (1998) Coordination geometries of selected transition metal ions (Co^{2+} , Ni^{2+} , Cu^{2+} , Zn^{2+} , Cd^{2+} and Hg^{2+}) in metalloproteins, *J. Inorg. Biochem.* 71, 115–127.
- Carrington, P. E., Chivers, P. T., Al-Mjeni, F., Sauer, R. T., and Maroney, M. J. (2003) Nickel coordination is regulated by the DNA-bound state of NikR, *Nat. Struct. Biol.* 10, 126–130.
- Phillips, S. E. V., Manfield, I., Parsons, I., Davidson, B. E., Rafferty, J. B., Somers, W. S., Margarita, D., Cohen, G. N., Saint-Girons, I., and Stockley, P. G. (1989) Cooperative tandem binding of *met* repressor of *Escherichia coli*, *Nature* 341, 711–715.
- Gangola, P., and Rosen, B. P. (1987) Maintenance of intracellular calcium in *Escherichia coli*, *J. Biol. Chem.* 262, 12570–12574.
- Cavet, J. S., Meng, W., Pennella, M. A., Appelhoff, R. J., Giedroc, D. P., and Robinson, N. J. (2002) A nickel-cobalt-sensing ArsR–SmtB family repressor, *J. Biol. Chem.* 277, 38441–38448.
- Guedon, E., and Helmann, J. D. (2003) Origins of metal ion selectivity in the DtxR/MntR family of metalloregulators, *Mol. Microbiol.* 48, 495–506.
- Waldburger, C. D., and Sauer, R. T. (1995) Domains of Mnt Repressor: roles in tetramer formation, protein stability, and operator DNA binding, *Biochemistry* 34, 13109–13116.
- Peña, M. M. O., Lee, J., and Thiele, D. J. (1999) Delicate balance: homeostatic control of copper uptake and distribution, *J. Nutr.* 129, 1251–1260.
- Rosenzweig, A. C. (2001) Copper delivery by metallochaperone proteins, *Acc. Chem. Res.* 34, 119–128.
- Hati, S., Boles, A. R., Zaborske, J. M., Bergman, B., Posto, A. L., and Burke, D. H. (2003) Nickel $^{2+}$ -mediated assembly of an RNA-amino acid complex, *Chem. Biol.* 10, 1129–1137.
- Cook, W. J., Kar, S. R., Taylor, K. B., and Hall, L. M. (1998) Crystal structure of the cyanobacterial metallothionein repressor SmtB: A model for metalloregulatory protein, *J. Mol. Biol.* 275, 337–346.
- VanZile, M. L., Chen, X., and Giedroc, D. P. (2002) Structural characterization of distinct $\alpha 3\text{N}$ and $\alpha 5$ metal sites in the cyanobacterial zinc sensor SmtB, *Biochemistry* 41, 9765–9775.

29. VanZile, M. L., Chen, X., and Giedroc, D. P. (2002) Allosteric negative regulation of *smt* O/P binding of the zinc sensor, SmtB, by metal ions: A coupled equilibrium analysis, *Biochemistry* 41, 9776–9786.
30. Jacquamet, L., Aberdam, D., Adrait, A., Hazemann, J.-L., Latour, J.-M., and Michaud-Soret, I. (1998) X-ray absorption spectroscopy of a new zinc site in the fur protein from *Escherichia coli*, *Biochemistry* 37, 2564–2571.
31. Althaus, E. W., Outten, C. E., Olson, K. E., Cao, H., and O'Halloran, T. V. (1999) The ferric uptake regulation (Fur) repressor is a zinc metalloprotein, *Biochemistry* 38, 6559–6569.
32. Outten, C. E., Tobin, D. A., Penner-Hahn, J. E., and O'Halloran, T. V. (2001) Characterization of the metal receptor sites in *Escherichia coli* Zur, an ultrasensitive zinc(II) metalloregulatory protein, *Biochemistry* 40, 10417–10423.
33. Spiering, M. M., Ringe, D., Murphy, J. R., and Marletta, M. A. (2003) Metal stoichiometry and functional studies of the diphtheria toxin repressor, *Proc. Natl. Acad. Sci. U.S.A.* 100, 3808–3813.
34. Love, J. F., vanderSpek, J. C., Marin, V., Guerrero, L., Logan, T. M., and Murphy, J. R. (2004) Genetic and biophysical studies of diphtheria toxin repressor (DtxR) and the hyperactive mutant DtxR(E175K) support a multistep model of activation, *Proc. Natl. Acad. Sci. U.S.A.* 101, 2506–2511.
35. Helmann, J. D. (2002) Sensing nickel: NikRs with two pockets, *Chem. Biol.* 9, 1055–1057.
36. Azam, T. A., Iwata, A., Nishimura, A., Ueda, S., and Ishihama, A. (1999) Growth phase-dependent variation in protein composition of the *Escherichia coli* nucleoid, *J. Bacteriol.* 181, 6361–6370.
37. Young, G. M., and Postle, K. (1994) Repression of *tonB* transcription during anaerobic growth requires Fur binding at the promoter and a second factor binding upstream, *Mol. Microbiol.* 11, 943–954.

BI049404K